Indian J. Phys. 78 (7), 591-598 (2004)

AN INTERNATIONAL JOURNAL
IJP

Electron-phonon resonance in some new charge transfer complexes

A T Oza*, G K Solanki, R G Patel and S M Prajapati

Department of Physics, Sardar Patel University,
Vallabh Vidyanagar-388 120, Gujarat, India

E-mail : headphys@spu.ernet.in

Received 16 December 2002, accepted 18 May 2004

Abstract Some new charge transfer complexes of organic donors and acceptors were prepared and the infrared spectra in the range 400-4000 cm^{-1} were obtained. The analysis of featureless absorption between the two envelopes at 1400 cm^{-1} and 3400 cm^{-1} were carried out for the transitions across the band gap. Six complexes show spectral characteristic of the presence of charge density waves. Electron–phonon resonance is found. Bands are ascribed to various intramolecular bond vibrations of donor and acceptors. Systematic distortion of the Gaussian band as the occurrence of electron - phonon resonance is discussed. Other four complexes show variation of the band gap.

Keywords Infrared spectra, charge transfer complexes, Gaussian bands, optical absorption edge, electron-phonon resonance

PACS Nos. 78.30.-j, 87.15.Mi

1. Introduction

There is a lot of interest among the solid state physicists to study the physical properties of organic charge transfer complexes and radical-ion salts. Among them, polyphenyl sulphide [1], hydroxymethyl-ferrocene [2], lithium phthalocyanine [3], pure phthalocyanine [4], poly (phenylene vinylene) [5], Ag-phenanthroline - TCNQ [6], poly (toluidine) [7] Mg-phthalocyanine [8], polyaniline [9,10], polybithiophene and polyterthiophene [11], quaterthiophene [12], *etc* are the examples. Photoconductivity and photovoltaic studies are made in view of finding applications in semiconducting devices. Novel organic semiconductors and nonlinear phenomena in organic solids are reviewed elsewhere [13, 14].

The purpose of the present work is to elucidate the electron phonon resonance in organic conductors through the infrared spectroscopy.

Experimental

Some new charge transfer complexes based on organic acceptors like 2, 3 - dichloro - 5 , 6 - dicyano - p - benzoquinone (D D Q), 7, 8, 8 - tetracyano - p - quinodimethane (TCNQ) and 2,4,5,7, - tranitro 9-flourenone (TNF) were prepared. Donors like N,N-phenyl-p-phenylenediamine (DPPD), pyridine, triethylamine and 2,2'-bipyridyl were used. Most of the donors and acceptors were ordered from Aldrich Chemical Co. (USA). TNF and TCNQ complexes were prepared by dissolving donors and acceptors in 1:2 molecular weight proportions in acetonitrile and then mixing the solutions for precipitation of solutions of charge transfer complexes. If a complex was soluble in acetonitrile, the solvent was allowed to evaporate out to leave the solid in the beaker. DDQ complexes were prepared in a similar manner using carbon tetrachloride as the solvent. Pyridine $(DDQ)_2$ and triethylamine $(DDQ)_3$ were prepared by mixing liquid donors with DDQ and stirring. These complexes and the colours of complexes are listed here (Table 1). Only pyridine - iodine is known [15].

The samples for infrared measurements were prepared by preparing colloidal suspension in paraffin oil or grinding KBr (dry powder) and the charge transfer complex together in a mortar. Only a little (below 5%) concentration of CT complex was used and grinded with KBr till the complex dispersed in a large amount of KBr. Semi-transparent pellets of size of 1.33 cm diameter and 2mm thickness were prepared by pressing in a die.

A double-beam infrared spectrophotometer (model : 983) of Perkin - Elmer Company, USA, was used. The resolution of this spectrophotometer was about 1 cm^{-1}. The results were accurate in the transmission mode and were reproducible.

*Corresponding Author

Table 1. Spectral properties of new charge transfer complexes.

Name of the charge transfer complexes	Colour	Absorption function	Type of transition	Optical absorption edge (ev)
DPPD $(TCNQ)_2$	Blue	$Ahv=B(hv-Eg)^{1/2}$	Allowed direct	0.2025
DPPD $(DDQ)_2$	Green	$Ahv=B(hv-Eg)^{1/2}$	Forbidden direct	0.285
Pyridine $(DDQ)_2$	Blue	$Ahv=B(hv-Eg)^{1}$	Forbidden indirect	0.225
Triethylamine $(DDQ)_2$	Red	$Ahv=B(hv-Eg)^{1/2}$	Forbidden Direct	0 2175
Benzidine $(TNF)_2$	Blue	$Ahv=B(hv-Eg)^{2}$	Allowed indirect	0 225
Bipyridy $(DDQ))_2$	Blue	$Ahv=B(hv-Eg)^{1/2}$	Forbidden direct	0.220
Pyridine-Iodine	Brassy	$Ahv=B(hv-Eg)^{1/2}$	Allowed direct	0 2175
Triethylamine $(TNF)_2$	Green	$Ahv=B(hv-Eg)^{1/2}$	Forbidden direct	0 225
Bipyridyl	Blue	$Ahv=B(hv-Eg)^{1/2}$	Allowed direct	0.220
DPPD$(TNF)_2$	Black	$Ahv=B(hv-Eg)^{1/2}$	Forbidden direct	0 220

3. Results and discussion

The infrared spectra of six complexes which show a broad and intense dip in the transmission around 1400 cm^{-1} are shown in Figures 1 and 2. Minimum transmission values and maximum 100-T (%) values are noted for the dip (Table 2). An envelope around 1400 cm^{-1} contains a large number of vibrational bands in optical conductivity [16-26]. The vibrational bands ride over and superpose a continuous background peak. This background peak which may be obtained by joining maximum transmission of sharp bands, *i.e.* by joining maximum 100-T values, may be due to reflection and scattering. Now since the materials are highly anisotropic and reflect only along one direction, the

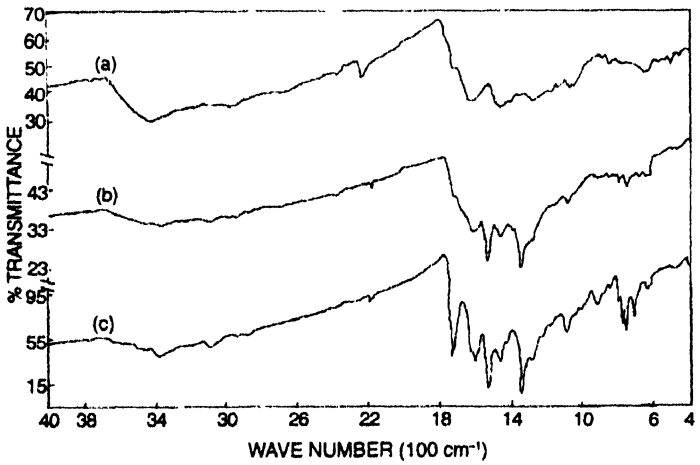

Figure 1. Infrared spectra of (a) TEtA $(DDQ)_2$ (b) TEtA $(TNF)_2$ and (c) Bip $(TNF)_2$

directional averaging will give more transmission than reflection because materials transmit light in two directions. Secondly, pellets contained only a little amount of charge transfer complex (less than 5%) and are grinded till it dispersed to form semi transparent pellets. So reflection was negligible. Also reflection of such one-dimensional conductor show a dip in the infrared

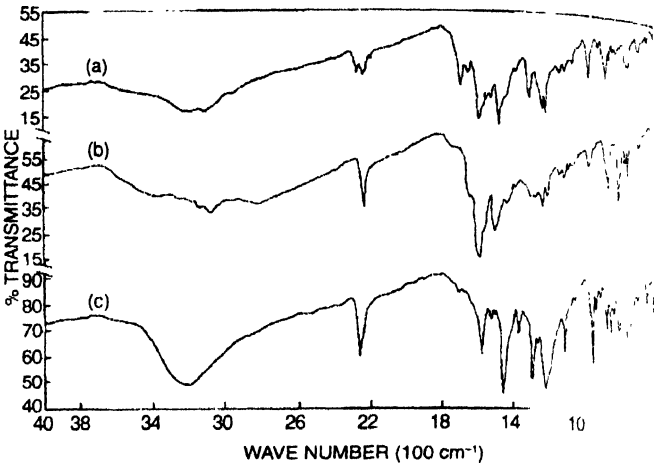

Figure 2. Infrared spectra of : (a) Bip $(DDQ)_2$; (b) Py I_2 , (c) Benzidi $(TNF)_2$ and (d) DPPD $(TNF)_2$

range and not a peak [27-29]. Also in highly conducting medium A=T and R=1-A or 1-T where A is absorbance, T is transmittance and R is reflectance. This is the case when thickness of the sample is much larger than the skin depth. Skin depth is very less for a highly conducting medium [30]. The skin depth will be very small when charge density waves are formed which lead high conductivity. Thus, the observed transmission dips can be considered to be electronic absorption envelopes rather th a reflection envelopes. The maximum reflectance curve show broad minimum which corresponds to a negative dip in the r part of dielectric constant and a broad maximum in the imagin part [28]. Such results are also found in the case of (DPPD) pyrene $(TNF)_2$ and perylene $(TNF)_2$ where the Kramers-Kro analysis was carried out [29]. Other four complexes do not sh any absorption envelope formation (Figure 3).

Table 2. Parameters of absorption envelope.

Name of the complex	No. of bands in the envelope (N)	Ln σ	Absorption strength (Ω^{-1} cm^{-2})	Optical conductiv (Ω^{-1} cm^{-1}
TEtA $(TNF)_2$	5	2.0	3.1×10^{-9}	7 39
TetA $(DDQ)_2$	6	2.4	4.62×10^{-9}	11 02
Bip $(DDQ)_2$	7	2.9	7.6×10^{-9}	18 17
DPPD $(DDQ)_2$	8	3.5	1.4×10^{-8}	33 12
Bip $(TNF)_2$	9	3.8	1.9×10^{-8}	44 70
Py$(DDQ)_2$	10	4.0	2.3×10^{-8}	54 60

In the six compounds, which show absorption envelop there is a strong possibility of showing charge density wav by other measurements like electrical conductivity. Resonanc

anti-resonance spikes around the envelope are also clearly observed. The inflexion points or mid-points can be joined to form a broad absorption envelope [28]. This graphical method gives more accurate values of optical conductivity profile. A third method is to consider a modulated wave-packet by joining sharp peak values of vibrational bands. The resonance -anti-resonance spikes are because of strong electron-phonon interaction which leads to the formation of charge density waves. Electronic motion couples with intra-molecular vibrations which leads to overall coupling constant.

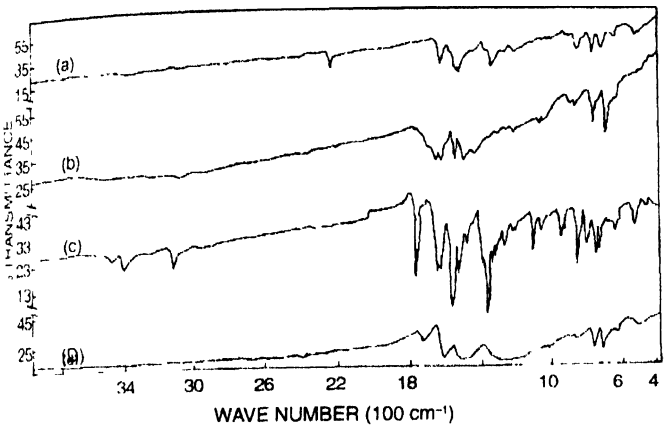

Figure 3. Infrared spectra of (a) DPPD $(TCNQ)_2$, (b) Py I_2, (c) Benzidine $(TNF)_2$ and (d) DPPD $(TNF)_2$

The density waves (both charge and spin density waves) are treated as broken symmetry of metals [30]. There is breaking of translational symmetry due to simultaneously damped and displaced oscillators interacting through long-range forces. The infrared spectra of $\sigma_1(\omega)$ (real part of complex conductivity) show one or two peaks in one-dimensional conductor [30] like TaS_3, $(TaSe_4)_2I$, $K_{0.3}MoO_3$, KCP-Br and $(TMTSF)_2PF_6$. The collective gap lies in FIR (far infrared) and microwave range while single particle gap lies in the infrared range [31] ; such a gap linearly scales with effective mass. $\sigma_1(\omega)$ is related with $\varepsilon_2(\omega)$ as discussed below.

A peak in absorption is also a peak in the imaginary part of dielectric constant which is in turn, related with lattice distortion. This may not be in general, valid for metals but it is valid for low-dimensional conductors which show Kohn anomaly and Peierls distortion. There is an increase (peak) in a.c. conductivity with a simultaneous decrease in d.c. conductivity, *i.e.* there is borrowing of oscillator strength from d.c. response.

Absorption coefficient (α) and imaginary part of dielectric constant (ε_2) are related to the optical conductivity (σ) through the relations [32],

$$\sigma(\omega) = \frac{\alpha(\omega) n_1(\omega) c}{4\pi} = \frac{\omega \varepsilon_2}{4\pi}. \qquad (1)$$

Here, n_1 is the real part of refractive index, c is the velocity of light, $n_1(\omega)$ is the monotonic function of frequency and therefore, peak in $\alpha(\omega)$ corresponds to peak $\sigma(\omega)$ and $\varepsilon_2(\omega)$. The optical conductivity also shows electronic envelope and resonance and anti-resonance spikes [28]. Absolute $\sigma(\omega)$ values are noted for the six complexes (Table 2). The absorption strength α in Ω^{-1} cm $^{-2}$ and optical conductivity (σ) in Ω^{-1} cm^{-1} were obtained by converting units from cm $^{-1}$ of α and sec $^{-1}$ of σ.

Band assignments in the infrared range were carried out with guidance from elsewhere [33,34]. Bands near 3400 cm $^{-1}$ was ascribed to N-H stretching in benzidine and N,N' - diphenyl-p-phenylenediamine (DPPD) complexes aromatic and heterocyclic system. 1320 cm^{-1} band was assigned other C-C vibrations. Band in 400-700 cm $^{-1}$ range were due to rocking and wagging modes as well as group vibrations. One or two may be Raman active modes particularly for the asymmetric molecules. Bands at 1500 cm^{-1} and 1300 cm^{-1} were ascribed to NO_2 stretching in TNF complexes. A band due to C-Cl vibration was also found in DDQ complexes. For comparison, the spectra of TCNQ, DDQ and TNF are shown in Figure 4. Several vibrational bands found to be broadened in charge transfer complexes (Figures 1 and 2).

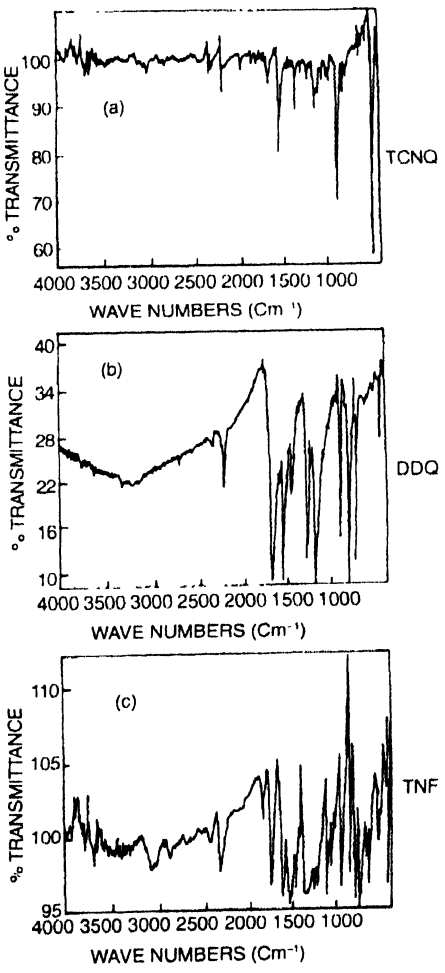

Figure 4. Infrared spectra of (a) TCNQ, (b) DDQ and (c) TNF.

When electronic motions couple with intramolecular vibrations, Rice's model is applicable and frequency shifts, particularly red-shifts, are expected due to electron-phonon

Table 3. Frequency shifts due to electron–phonon coupling.

Compound No.	Name of the complex	Shifted band (cm^{-1})	Unshifted band only in acceptor (cm^{-1})
1	$TEtA(TNF)_2$	1620	1460
		1550	1395
		1480	1330
		1360	1225
		1100	990
2	$TEtA(DDQ)_2$	1750	1575
		1600	1440
		1480	1330
		1420	1280
		1370	1235
		1280	1150
3	$Bip\ (DDQ)_2$	1700	1530
		1650	1485
		1600	1440
		1500	1350
		1400	1260
		1300	1170
		1220	1100
4	$DPPD\ (DDQ)_2$	1590	1430
		1500	1350
		1460	1315
		1370	1235
		1285	1164
		1270	1145
		1200	1080
		1085	987
5	$Bip\ (TNF)_2$	1730	1595
		1600	1440
		1540	1385
		1470	1325
		1360	1225
		1300	1170
		1200	1080
		1095	985
		910	820
6	$Py(DDQ)_2$	1600	1440
		1510	1360
		1430	1290
		1380	1240
		1270	1145
		1200	1080
		1170	1050
		1080	970
		1050	945
		900	810

coupling. The shift depends on the coupling constant and other quantities. This is observed in TCNQ complexes [28]. Here, the complexes showing an envelope formation are DDQ and TNF complexes. Bands in only DDQ and TNF as well as those of there complexes are listed here to visualize the frequency shifts (Table 3). These shifts which lie in the infrared range are related with Kohn anomaly. The dispersion curves of acoustic and optical phonons lie in 10^{12} Hz [35] range and infrared range is $10^{11} - 10^{13}$ Hz [28]. The Kohn anomaly occurs when there is anisotropic (ellipsoidal or cylindrical) Fermi surface [36, 37]. It is a dynamic anomaly which results in a Peierls distortion of a linear metallic chain at low temperatures or whenever a perturbation is applied [38]. The frequency of $q = 2K_F$ vibration reduces and there is softening of a phonon mode. q is phonon wave vector and K_F is electron wavevector corresponding to the Fermi level.

It should be noted that Gaussian bands found in TEtA $(DDQ)_2$ (Figures 1a and 5) and DPPD $(DDQ)_2$ (Figures 2c and 5) are slowly being distorted in other complexes as charge transfer interaction and consequently electron-phonon interaction becomes stronger. A Gaussian curve obeys

$$A = A_0 \exp\text{-}\ \frac{(\omega - \omega_0)^2}{2M_2}$$

where A is the absorbance, A_0 is the maximum absorbance, ω_0 is the central frequency and M_2 is the second moment of the distribution. Thus, lnA *vs* $(k - k_0)^2$ is a straight line. TEtA $(TNF)_2$

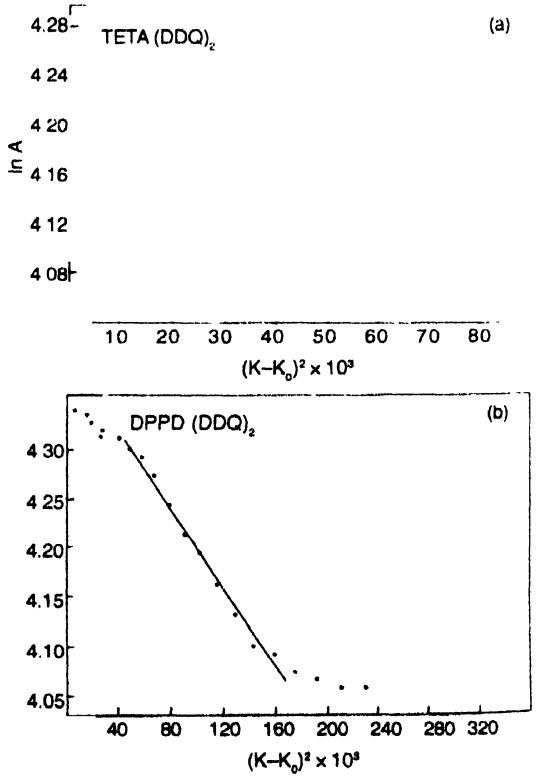

Figure 5. Gaussian at 3400 cm^{-1} in (a) TEtA $(DDQ)_2$ and (b) DPPD $(DDQ)_2$.

(Figure 1b) and Py(DDQ)$_2$ (Figure 2b) are intermediate cases in which two phonon bands remain at somewhat lower frequencies than the Gaussian curves and a result half of the Gaussian curve on high frequency side only is retained. Then comes Bip(TNF)$_2$ (Figure 1c) in which two phonon bands superpose a weak and broad Gaussian profile. Here the interaction is weak and overall Gaussian curve can be deconvoluted. The distortion of complete Gaussian curve is observed in Bip(DDQ)$_2$ (Figure 2a). When two phonon bands come nearer to the Gaussian profile, electron-phonon resonance takes place and Gaussian curve becomes a degenerate oscillator. These results should be compared with the spectra of strongly interacting donors and acceptors in which two oscillator model fits well [28]. Thus there is electron-phonon resonance in which the oscillator model appears when the electronic motions match the frequency of soft phonon modes

The contribution from free carriers to the dielectric constant is given by [39]

$$n^2 - k^2 = \frac{Ne^2}{m^* \varepsilon_0} \frac{\tau^2}{1+\omega^2\tau^2} = \frac{\varepsilon}{\varepsilon_0} \tag{3a}$$

and

$$2nk = \frac{Ne^2}{m^* \varepsilon_0} \frac{\tau}{\omega\left(1+\omega^2\tau^2\right)} = \frac{\sigma}{\omega\varepsilon_0}. \tag{3b}$$

Here, N is the number of oscillators, m^* is the effective mass and τ is the relaxation time. Also e is the electronic charge, ε_0 is the dielectric constant of air, ω is the frequency of incident radiation and σ is the optical conductivity.

n is the real part of the refractive index and k is the imaginary part of the refractive index $n^2 - k^2$ is a Cauchy distribution in frequency.

For damped - driven oscillator [39],

$$n^2 - k^2 = 1 + \frac{Ne^2}{m^* \varepsilon_0} \frac{\left(\omega_0 - \omega\right)^2}{\left(\omega_0^2 - \omega^2\right)^2 + \left(\omega\beta/m^*\right)^2} \tag{4a}$$

and

$$2nk = \frac{Ne^2}{m^* \varepsilon_0} \frac{\omega\beta/m}{\left(\omega^2 - \omega^2\right)^2 + \left(\omega\beta/m^*\right)^2}. \tag{4b}$$

Here, β is the damping coefficient, m^* is the effective mass and ω_0 is the resonance frequency and these are known as Hanle curves. $n^2 - k^2$ has a dispersion shape and 2nk has a resonance line-shape. These eqs. (2a), (2b), (3a) and (3b) are obtained from electronic polarizability. Similar equations hold for ionic polarizability but the natural frequency ω_0 lies in the infrared range [39].

A phenomenological mode [40] of charge density waves when there is electron-phonon coupling is discussed in which there is damped driven oscillator is considered.

$$\varepsilon_F(\omega) = 1 + \frac{\omega_p^2 (n_s/n)(m/m^*)}{\omega_F^2 - \omega^2 - i\Gamma\omega}. \tag{5}$$

ω_p is the plasma frequency, n_s is the no. of condensed electrons, ω_F is the pinning frequency and Γ is damping coefficient.

When $\Gamma = 0$ (no damping), this $\sigma_F(\omega)$ leads to the London equation for superconductivity.

It can also be concluded from the spectra that TCNQ and DDQ are stronger acceptor and give highly conducting complexes than TNF and I_2. It should be noted that TCNQ and DDQ have negative and reversible half wave reduction potentials. The spectra of TCNQ and DDQ complexes are nearer to those of completely ionic salts than those of TNF and I_2 complexes. Bands of TCNQ- are observed in DPPD (TCNQ)$_2$ (Figure 3a) below 1670 cm^{-1} and the complex is supposed to be a Hubbard insulator like alkali TCNQ salts. Complete ionization means strong Coulomb repulsion along stacks and a perfectly half-filled band and this is the reason for its insulating nature. Semiquinone ion bands are found in the spectra of DDQ complexes at 11.3μ, 9.5μ, 8.4μ and 8.2μ which shows ionic nature. For TNF and I_2, interaction is weak and an electronic Gaussian envelope remains without tailing towards low frequency side or any distortion to degenerate oscillator. A donor band due to N-H or N-CH$_3$ bond at 2200 cm^{-1} is found to be strong in TCNQ and DDQ complexes than TNF and I_2 complexes.

The relation between absorption coefficient and the optical conductivity is $\sigma(\omega) = \alpha n_1 c / 4\pi$ and therefore, $n_1(\omega)$ plays role in determining the envelope around 1400 cm^{-1} in $\sigma(\omega)$, $n_1(\omega)$ has a dispersion line shape in the region of anomalous dispersion. This will give rise to a tailing of the envelope towards low frequency side and the envelope does not remain symmetric. This is observed in all the optical conductivity spectra of six complexes for the envelope around 1400 cm^{-1}. In spite of n_1 leading to a band tail towards low frequency side, the envelope behaviour of $n_2 = \varepsilon_1\varepsilon_2$ (*i.e.* k - the imaginary part of refractive index).

In Bip (DDQ)$_2$ and Py (DDQ)$_2$, the charge transfer interaction is very strong and consequently, electron-phonon interaction is also strong. As a result, the envelope at 1400 cm^{-1} is splitted into two small envelopes around 1600 cm^{-1} and 1200 cm^{-1}. There is a quadrupole splitting of about 400 cm^{-1}. Thus, the conduction band seems to be split. Such a three-envelope situation is found in some complexes by other workers also.

There are large number of bands in the spectra of all ten complexes because of mixing of intermolecular and intramolecular phonon modes. The intermolecular phonons are based on the crystal structures of the materials. The major role in determining

infrared profile is played by intramolecular bond vibrations in organic charge transfer complexes.

The spectra of purely organic complexes are found to be different from charge transfer complexes of transition metal chelates [41,42]. Here band assignment (Table 3) is possible because the intramolecular vibrations dominate while in the complexes of electron donating metal chelates intermolecular phonons and mixing of donor and acceptor bands with large blue and red shift mainly occurs due to very weak polarization of donor and its organic network.

The Gaussian curve found in $(TCNQ)_2$ and DPPD $(DDQ)_2$ around 3400 cm^{-1} should be compared with the Gaussian curve found in UV-visible spectra of organic polyiodide chain complexes [43, 44]. These Gaussian bands were explained on the base broadening by Raman active phonon modes. Here, the resonance occurs when electronic absorption and phonon band coincide in frequency and Gaussian band becomes a degenerate oscillator. The relation between an oscillator model and Gaussian curve is recently established when the damping coefficient is large [45]. There is electron-phonon resonance. In polyiodide chain complexes, phonon bands in far-infrared range broaden Gaussian profile in UV-visible range [43, 44]. Electron-phonon coupling seems to be of different type. In the six charge transfer complexes of the present study, phonon bands associated with intramolecular vibrations are broadened by free electronic motions. Consequently, electronic absorption changes from a Cauchy distribution to Gaussian distribution.

There is a range between 3700 cm^{-1} and 4000 cm^{-1} in which the absorption increases as wavelength increases in all six complexes. The range is very small for complete analysis and near-infrared spectra are required. But a checking of this range shows that the free charge carriers are scattered by acoustic phonons because $\alpha_f = A\lambda^{1.5}$ where α_f is the free carrier absorption coefficient, λ is the wavelength of infrared light and A is a constant. Free carrier absorption is discussed elsewhere [46].

The envelope at 1400 cm^{-1} mainly contain a large number of acceptor bands due to intramolecular vibrations and is therefore, related with the ionic state of organic acceptor due to charge transfer. The envelope at 3400 cm^{-1} is connected with the polarization of donors which remain Gaussian curve when the interactions are weak and becomes degenerate oscillator when interactions are strong.

In DPPD $(TCNQ)_2$ (Figure 3a), TCNQ bands are observed which are a_g symmetric vibrational bands. The bands below 700 cm^{-1} are red-shifted due to softening of these phonon bands. The bands above 700 cm^{-1} are blue-shifted due to anharmonic interactions. Moreover, three or four doublets found in the range between 700 cm^{-1} and 1600 cm^{-1} are completely split and observed as separate bands with blue shifts. There are group vibrations outside the ring in TCNQ which give rise to bands below 70 cm^{-1}. Raman-active modes which also lie in the range, are n possible because of symmetry of the molecule. Thus, grou vibrations become soft due to charge transfer. Othe intramolecular bond vibrations become hard and are blue-shifte because of anharmonic interactions with electronic motions

Electronic transitions across the single particle band gap whether these transitions are direct or indirect and forbidden o allowed, are analyzed here in ten complexes and are summarize in four figures (Table 1 and Figures 6-9). Here, we treat the singl

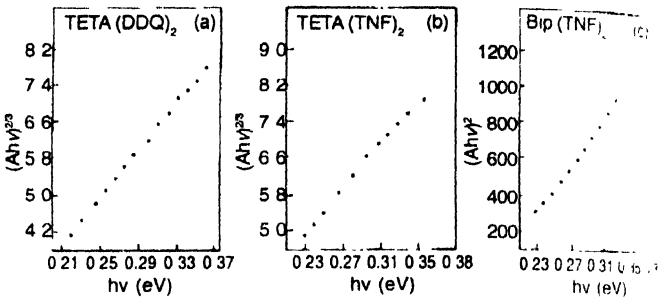

Figure 6. (a) Transition in TEtA $(DDQ)_2$, (b) Transition in TEtA $(TNF)_2$ and (c) Transition in Bip $(TNF)_2$

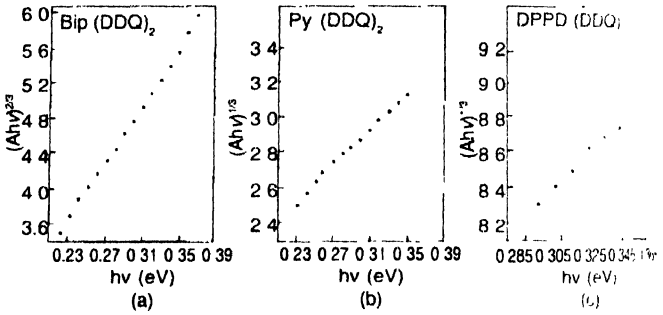

Figure 7. (a) Transition in Bip $(DDQ)_2$, (b) Transition in Py $(DDQ)_2$ and (c) Transition in DPPD $(DDQ)_2$.

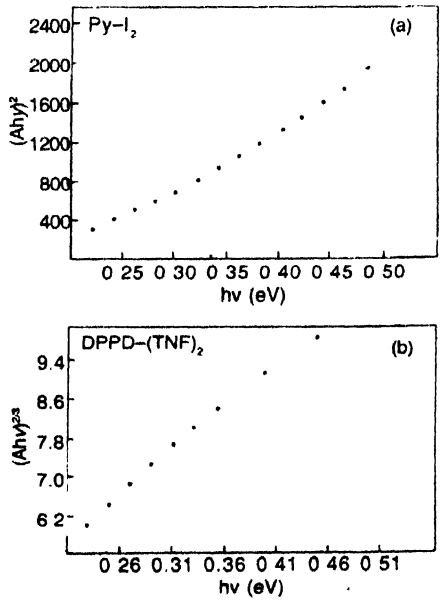

Figure 8. (a) Transition in $Py\text{-}I_2$ and (b) Transition in DPPD $(TNF)_2$

particle Peierls gap as an ordinary band gap as in the case of an elemental or compound (inorganic) semiconductor and consider $(\alpha h\nu)^2 B(h\nu - Eg)^r$ using $r = ½$ for direct transition and $r = 2$ for indirect transition. $r = 3/2$ for forbidden direct transition, $r = 3$ for forbidden indirect transition for this $(\alpha h\nu)^{1/r}$ *vs* $h\nu$ is plotted [46]. All these dependencies are also found in the ten charge transfer complexes studied here. The details of such transitions are discussed elsewhere [46]. All these dependencies are also found in the ten charge transfer complexes studied here. The details of such transitions are discussed elsewhere [29, 47]. All possible functions were computed and plotted and only best fit are shown here (Figures 5-8). It should be noted that all ten purely organic complexes studied here, show direct transitions (Table 1) and ten complexes of organometallic chelates $Ni(Hdmg)_2$, $Ni(Hdpg)_2$ and PbPc, where dmg=dimethylglyoxime, dpg = diphenylglyoxime and Pc = Phthalocyanine show indirect transitions [41,42]. This difference is important. It can be concluded that metal ligand vibrations in the charge transfer complexes of metal-organic chelates play important role in the absorption and emission of a phonon during a transition between the valence and conduction band. Such analysis was done earlier also.

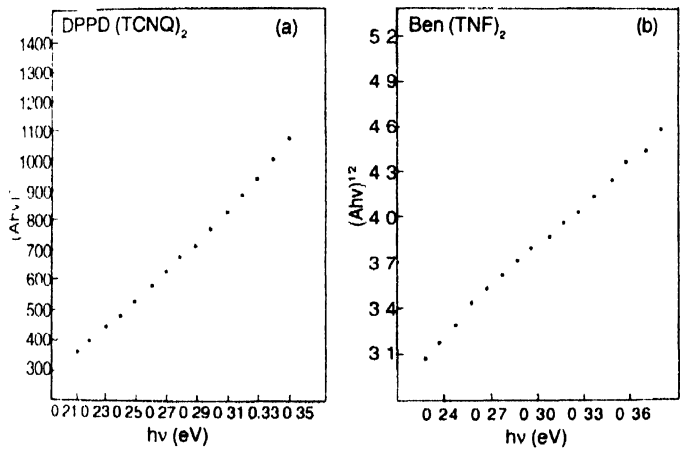

Figure 9. (a) Transition in DPPD $(TCNQ)_2$ and (b) Transition in benzidine $(TNF)_2$

Alternatively, the complicated spectra were found because of harmonic generations. General non-linear system which satisfy [48].

$$\ddot{X} + \omega_T^2 X = \mu F(\omega_4, X, X), \tag{6}$$

vibrates at various frequencies given by $p\omega d + q\omega_T$ [43] where ω_d and ω_t are driving and pinning frequencies of donor and acceptor respectively and p and q are integers. If $p + q$ is even number, there is second harmonic generation and if $p + q$ is multiple of three, there is third harmonic generation. The calculated frequencies $p\omega_d + q\omega_T$ were found to fall within 5 cm^{-1} around observed frequencies for the six complexes showing CDW (charge density wave) features. A donor vibration around 3200 cm^{-1} starts driving a pinning vibration of counter ion (acceptor) which occurs around 1500 cm^{-1}. Various harmonics are generated through a push-pull mechanism because of intermolecular interactions. There is elasticity in pinning vibration. The charge transfer binding interaction, *i.e.* charge transfer contact moves in a lattice when CDWs are depinned

An electron is transferred to a neighboring molecule by flinging by intramolecular vibration. The vibration delocalized charge carriers. The number of vibrations coupled with the electronic motion (N), *i.e.* number of bands in the envelope around 1500 cm-1 forms a straight line with optical conductivity calculated from the absorption maximum of the envelope (log σ) (Figure 10 and Table 2). It should be noted that some time ago, log σ *vs* N for directly measured d.c. conductivity for 10 complexes was found to be a straight line. Here, optical conductivity in the infrared range gives a straight line. Thus, this straight line is frequency-independent. It is possible that optical conductivity shows a linear scaling relation with d.c. conductivity. The slope of such a straight line depends upon the end groups in the charge transfer complexes of organometallic chelates [38,39] while in purely organic complexes studied in the present case, the slope does not depend upon the end group. The reason remains unknown. Other four complexes which do not show absorption envelopes (Figure 3) also do not show any frequency shifts of bands and resonance anti-resonance spikes. These are ordinary semiconductors and one–electron theory is applicable. There is no electron–phonon coupling and consequent formation of CDWs. Gaussians bands found in other six complexes at 3400 cm^{-1} are completely missing in the four complexes (Figure 3).

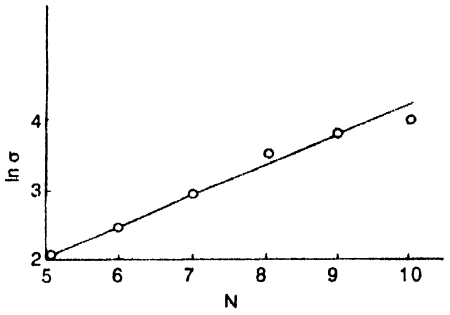

Figure 10. Ln *vs* N (number of coup vibrations) Is optical conductivity.

The Peierls gap in six complexes showing an increase in imaginary part of dielectric constant associated with lattice distortion, is of the order of 0.225eV. There is no variation of Peierls gap. In other four complexes, which do not show both of the envelopes, there is systematic variation of the band and this variation is noted (Table 4). Peierls gap of 0.225 ev is a universal band gap while semiconducting band gap arising from other aspects like Mott insulator, Hubbard insulator or an excitonic insulator is not universal and liable to change depending upon the molecular interactions. This is revealed in Table 5.

Table 4. Variation of band gap.

Name of complex	Band gap (eV)
DPPD $(TCNQ)_2$	0 2025
Py-I_2	0.2175
DPPD $(TNF)_2$	0.2200
Benzidine $(TNF)_2$	0.225

Acknowledgment

The authors are thankful to the University Grants Commission for Special Assistance Programme of DRS Scheme, under the auspices of which this experimental work was carried out.

References

[1] S H Kang, V Y Lee, J S Lee, K J Lim and M Zahn *1988 IEEE International Symposium of Electrical Insulation* (Cat No. 98, CH36239) **1** 210 (1998)

[2] A K Chakraborty, R N Bera, A Bhattacharjee and B Mallik *Synth. Met.* (Switzerland) **97** 63 (1998)

[3] M Brikmann, C Chaumont and J J Andre *Thin Solid Films* **324** 68 (1998)

[4] M Uurbanczya *J. Tech Phys* (Poland) **39** 275 (1998)

[5] H Becker, S E Burns and G J Denton *Cavandish Sympsium* (Boston, MA, USA 1–5 Dec.) (p.3) (1997)

[6] A Arena, S Pentene and G Saita *Nuovo Cim* (Italy) **D20** 907 (1998)

[7] J Ananda, S Palaniappan and D N Sathyanarayana *Polymer* (UK) **39** 6819 (1998)

[8] K P Krishnakum and C S Menon *Indian J Pure and Appl. Phys* **36** 342 (1998)

[9] J Lin, P J Kinlen and C R Graham *Cavandish Symposium* (Boston, MA USA, 1-5 Dec) p.623 (1997)

[10] V A Tabhane, A D Rangari and S Dhakate *Indian J. Pure and Appl Phys.* **36** 354 (1998)

[11] S Sato, M Fujitsuka, H Segawa, T Schimadzu and K Tananka *Synth. Met.* (Switzerland) **95** 107 (1998)

[12] W A Schoonveld, J Vrijmoeth and T M Klapwijk *Appl. Phys Lett* (USA) **73** 3884 (1998)

[13] H Inokuchi *Mol. Cryst. Liq. Cryst.* **216** 209 (1992)

[14] T Koda *Mol. Cryst. Liq Cryst.* **216** 139 (1992)

[15] M V Belousov, A M Vainrub and R M Valasova *Fiz Tuerd. Tela* (Leningrad) **19** 2637 (1976)

[16] M V Belousov, A M Vainrub, R M Valosova and V N Semkin *Fiz Tuerd Tela* (Leningrad) **20** 107 (1978)

[17] M G Kalpunov, T P Panova and V G Borodko *Phys. Stat. Sol* **A13** 1267 (1972)

[18] A Brau, P Bruesch, J P Farges, W Hinz and D Kuse *Phys. Stat. Sol.* **B62** 615 (1974)

[19] M J Rice, C B Duke and N O Lipari *Solid State Commun* **17** 1089 (1975)

[20] M J Rice, L Peitronero and P Bruesch *Solid State Commun* **21** 757 (1977)

[21] J Petzelt, K Kral, N Rysava, L Dobiasova, J Kroupa, J Oswald, A Szyskovskii and A Graja *Solid State Commun.* **32** 1315 (1979)

[22] M J Rice *Phys. Rev. Lett.* **37** 36 (1976)

[23] M J Rice in *Proc. Int. Cof. On Quasi – one – dimensional conductors*, Dubrovinik, Lecture Notes in Physics 96 (eds) Barisic *et al* (Berlin : Springer) (p.230) (1978)

[24] H Gutfreund, B Horrovitz and P Bruesch *J. Phys* **7** 383 (1974)

[25] T Kondow and T Sakata *Phys. Stat. Sol.* **6** 551 (1971)

[26] F Deveroux, M Neschtschein and G Gruner *Phys Rev Lett* **45** 53 (1980)

[27] P Bruesch *Proc. German Phys. Soc Conf On One dimensional Conductors* (saarbrucken) Lecture notes in Physics, **34** (ed H G Schuster) Springer - Berlin, July, 1974 (P.194)

[28] Ajay T Oza *Aust. J. Phys.* **42** 203 (1989)

[29] K D Patel and A T Oza *Indian J. Phys.* **71B** 161 (1997)

[30] Martin Dressel and George Gruner *Electridynamics of solids* (Cambridge University Press, U K) (2002) (p45, p173, p289)

[31] G Gruner *Density waves in solids* (Reading, MA : Addision Wesley) (1994)

[32] A O E Animalu *Intermediate Quantum Theory of Crystalline Solids*, (New Delhi Prentice Hall) (1978)

[33] Russel Drago *Physical Methods in Inorganic Chemistry* (New Delhi East - West Press) p222 (1965)

[34] P S Sindhu *Molecular Spectroscopy* (New Delhi Tata McGraw Hill) (1985)

[35] C Kittel *Introduction to Solid State Physics* 6th edn (Singapore : John Wiley) (1991)

[36] W Kohn *Phys Rev Lett.* **2** 393 (1959)

[37] A M Afanasev and Y U Kagan *Sov Phys JETP* **16** 1030 (1963)

[38] A T Oza and P C Vinodkumar *Indian J Phys.* **72A** 171 (1998)

[39] S Wang *Solid State Electronics* (New Delhi McGraw-Hill) (p651, 651, 398) (1965)

[40] M J Rice, S Strassler and W R Schneider in *Proc German Phys Soc Conf. On One-dimensional Conductors* (Saarbrucken) Lecture Notes in Physics 34 (ed) H G Schuster) (Berlin Springer) July (p 282) (1974)

[41] R G Patel and A T Oza *Indian J. Phys* **74A** 31 (2000)

[42] A T Oza, S G Patel, R G Patel, S M Prajapati and Rajiv Vaidya *Thin Solid Films* (accepted) (Abstract B-8-22-p, *Int Conf Mater Adv. Tech* (ICMAT), 7-12 Dec , Singapore, p73, 2003)

[43] E Mulazzi, L Piseri, I Pollini and R Tubino *Phys Rev* **B24** 3555 (1981)

[44] A T Oza *Thin Solid Films* **142** 153 (1986)

[45] A T Oza *Canad. J Phys* **80** 1175 (2002)

[46] A T Oza *Solid Stat. Commun* **71** 1005 (1989)

[47] R S Kireev *Semiconductor Physics* (Moscow : Mir) p537 (1979)

[48] Nicholas Minorsky *Non-Linear Oscillations* (D Van Nostrand) (p735, p741) (1982)